How to cite: Angew. Chem. Int. Ed. 2023, e202314977
doi.org/10.1002/anie.202314977

Hybrid Metal Halides

0D Pyramid-intercalated 2D Bimetallic Halides with Tunable Electronic Structures and Enhanced Emission under Pressure

Yang Liu, Jiayuan Liang, Zeyu Deng, Songhao Guo, Xiaoqin Ji, Congcong Chen, Pieremanuele Canepa, Xujie Lü,* and Lingling Mao**

Abstract: Hybrid metal halides are emerging semiconductors as potential candidates for optoelectronics. The pursuit of hybridizing various dimensions of metal halides remains a desirable yet highly complex endeavor. By utilizing dimension engineering, a diverse array of new materials with intrinsically different electronic and optical properties has been developed. Here, we report a new family of 2D-0D hybrid bimetallic halides, $(C_6N_2H_{14})_2SbCdCl_9\cdot 2H_2O$ (**SbCd**) and $(C_6N_2H_{14})_2SbCuCl_9\cdot 2H_2O$ (**SbCu**). These compounds adopt a new layered structure, consisting of alternating 0D square pyramidal $[SbCl_5]$ and 2D inorganic layers sandwiched by organic layers. **SbCd** and **SbCu** have optical band gaps of 3.3 and 2.3 eV, respectively. These compounds exhibit weak photoluminescence (PL) at room temperature, and the PL gradually enhances with decreasing temperature. Density functional theory (DFT) calculations reveal that **SbCd** and **SbCu** are direct gap semiconductors, where first-principles band gaps follow the experimental trend. Moreover, given the different pressure responses of 0D and 2D components, these materials exhibit highly tunable electronic structures during compression, where a remarkable 11 times enhancement in PL emission is observed for **SbCd** at 19 GPa. This work opens new avenues for designing new layered bimetallic halides and further manipulating their structures and optoelectronic properties via pressure.

Introduction

Halide perovskites have attracted much attention in recent years due to their excellent photophysical properties and high potential in various optoelectronic applications, such as solar cells,[1] light-emitting diodes,[2] lasers,[3] etc. They can be designed to combine a variety of inorganic and organic components and show the advantages of easy processing and structural tunability.[4] Pb-based halide perovskites are the most extensively studied materials, but considering the toxicity of lead, the replacement of lead with non- or less-toxic metals is topic of major importance.[5] One common approach is the equivalent substitution by elements in the same group (Sn^{2+} and Ge^{2+}).[6] However, these 2+ metals are easily oxidized with poor stability, and impeding their use in practical applications. Alternatively, heterovalent substitution can be adopted to obtain new three-dimensional (3D) halide double perovskites (DPs) $A_2M^IM^{III}X_6$ with multiple combinations, where M^{III} are the trivalent cations Sb^{3+}, Bi^{3+}, In^{3+}, Ln^{3+}, Au^{3+}, etc. and M^I are monovalent cations Ag^+, Au^+, Li^+, Na^+, K^+, $CH_3NH_3^+$ (MA^+), etc.[7] In 1922, $Cs_2AuAuCl_6$ and $Cs_2AgAuCl_6$, have been discovered by Wells.[8] In 2016, Slavney et al.[9] and McClure et al.[10] simultaneously reported semiconducting halide double perovskite $Cs_2AgBiBr_6$ for potential use in photovoltaics. Since then, research revolving around halide DPs is on its way, and many fascinating compounds, such as $Cs_2AgSbCl_6$,[11] $Cs_2AgInCl_6$,[12] $(MA)_2KBiCl_6$ and $(MA)_2AgBiBr_6$ have been reported.[7b,f]

Inspired by the hybrid-layered 2D-halide perovskites, layered halide DPs have also attracted much attention.[13] The first hybrid layered halide DPs $(BA)_4AgBiBr_8$ and $(BA)_2CsAgBiBr_7$ were synthesized by incorporating buty-

[*] Dr. Y. Liu, Dr. X. Ji, C. Chen, Prof. Dr. L. Mao
Department of Chemistry, SUSTech Energy Institute for Carbon Neutrality, Southern University of Science and Technology
Shenzhen, Guangdong 518055 (P. R. China)
E-mail: maoll@sutech.edu.cn

J. Liang, Dr. S. Guo, Prof. Dr. X. Lü
Center for High Pressure Science and Technology Advanced Research (HPSTAR)
Shanghai 201203 (P. R. China)
E-mail: xujie.lu@hpstar.ac.cn

Dr. Z. Deng, Prof. Dr. P. Canepa
Department of Materials Science and Engineering, National University of Singapore
9 Engineering Drive 1, Singapore 117575 (Singapore)
E-mail: msedz@nus.edu.sg

Prof. Dr. P. Canepa
Singapore-MIT Alliance for Research and Technology
1 CREATE Way, 10–01 CREATE Tower, Singapore 138602 (Singapore)
and
Department of Chemical and Biomolecular Engineering, National University of Singapore
4 Engineering Drive 4, Singapore 117585 (Singapore)
and
Department of Electrical and Computer Engineering, and Texas Center for Superconductivity, University of Houston
Houston, TX 77204 (USA)

lammonium (BA) cations into the 3D $Cs_2AgBiBr_6$.[13c] Jana et al. reported the first iodide layered DP, $[AE2T]_2AgBiI_8$ (AE2T = 5,5′-diylbis-(amino-ethyl)-[2,2′-bithiophene]), with an optical band gap of 2.0 eV.[14] More examples of layered halide DPs with tunable band gaps have been reported by introducing different organic moieties.[15] On one hand, the dimensional reduction of 3D DPs to form 2D analogs seems to be a universal strategy and generates many new materials. On the other hand, the case of combining M^{II} and M^{III} in a DP system appears much rarer. Vargas et al. first incorporated Cu^{2+} and Sb^{3+} into layered chloride DP $Cs_4CuSb_2Cl_{12}$,[16] which exhibits high stability with a direct band gap of 1.0 eV. Subsequently, a family of $Cs_4M^{II}M^{III}Cl_{12}$ was investigated (M^{II}=Cu, Mn, Cd; M^{III}=Bi, Sb).[17] However, achieving M^{II}/M^{III} hybrid 2D bimetallic halides appears unpractical, since M^{II} and M^{III} will easily decompose into their respected halides, which means that the targeted phase either does not form or exists in a multiphasic regime. To elucidate the structure-property relations and identifying phases, high-pressure is a unique handle to access new materials and vastly unexplored chemical spaces.[18] For example, $(BA)_4AgBiBr_8$ showed pressure-induced photoluminescence with the rotation of $[MBr_6]$ (M=Bi, Ag) octahedra.[19] Yang et al. demonstrated $Cs_4M^{II}Bi_2Cl_{12}$ (M^{II}=Cd, $Cd_{0.8}Mn_{0.2}$, Mn) retains a metastable phase after the complete release of pressure.[20]

Here, we report two new M^{II}/M^{III} hybrid 2D bimetallic halides (Figure 1) and explore their atmospheric and high-pressure optical properties of these phases. Using DABCO (DABCO = 1,4-diazabicyclo[2.2.2]octane) as the templating cation, we successfully synthesized two M^{II}/Sb (M^{II}=Cd, Cu) hybrid 2D bimetallic halides, $(DABCO)_2SbCdCl_9\cdot 2H_2O$ (**SbCd**) and $(DABCO)_2SbCuCl_9\cdot 2H_2O$ (**SbCu**). These isomorphic compounds contain two distinct inorganic layers, where one layer consists of corner-sharing $[SbCl_6]$ octahedra and $[M^{II}{}_2Cl_{10}]$ dimers, and the other layer of isolated square-bipyrimidal $[SbCl_5]$ units. Changing the M^{II} site from Cd^{2+} to Cu^{2+}, the optical band gap decreases from 3.26 to 2.23 eV. Both compounds exhibit temperature-dependent photoluminescence (PL), where **SbCu** shows a PL quenching phenomenon, which can further be explained by the higher energy position of the Cu 3d orbitals. In situ high-pressure optical measurements reveal that only **SbCd** displays pressure-induced emission enhancement by about 11 times at ≈19 GPa compared with atmospheric PL. Our work underlines the significance of exploring new material spaces with complex structures and compositions, and provides unique insights into the property regulations through pressure.

Results and Discussion

The hybrid 2D bimetallic halides $(DABCO)_2SbM^{II}Cl_9\cdot 2H_2O$ (M^{II}=Cd, Cu) reported here were synthesized by mixing stoichiometric $SbCl_3$, $M^{II}Cl_2$ (M^{II}=Cd, Cu) and DABCO in HCl solution under heating and stirring to boil. However, other attempts to switch the M^{III} site to Bi^{3+} or In^{3+} were not successful. This could be due to the role of the second inorganic layer of square-bipyrimidal $[SbCl_5]$, whereas for Bi^{3+} and In^{3+} it is not a common geometry.

The crystallographic structures were determined by single-crystal X-ray diffraction.[21] Isostructural **SbCd** and **SbCu** both crystallize in tetragonal space group *P4/ncc*. The structure of **SbCd** was previously deposited in the CCDC (1025918) as a private communication and no related characterization has been reported. The layered structure contains two inorganic layers (I and II) and one organic layer, arranged in the order of inorganic layer I, organic layer, inorganic layer II… as shown in Figure 2. Only the inorganic layer I contains two kinds of metal octahedra

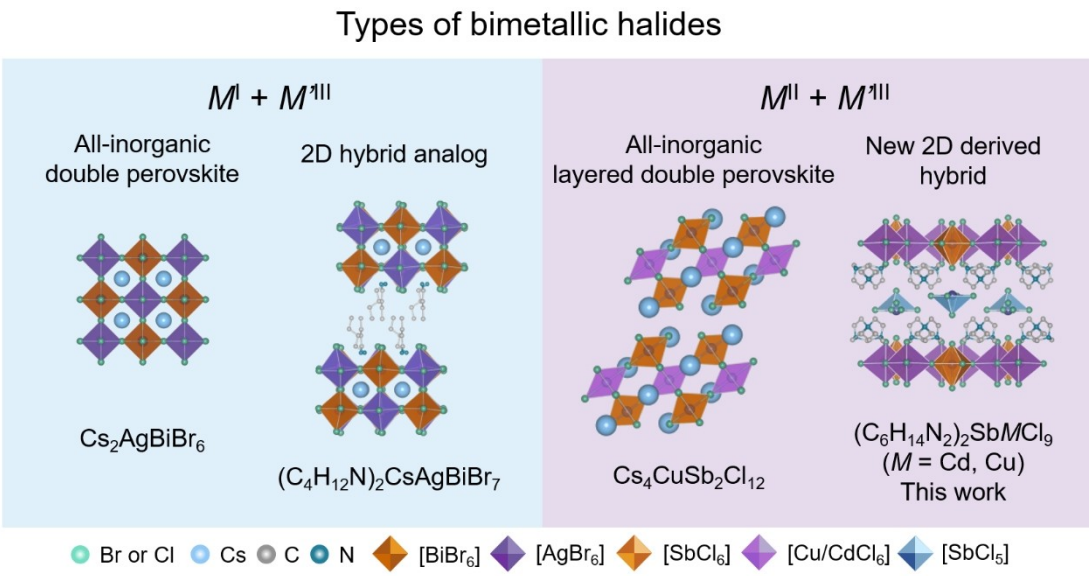

Figure 1. Representative bimetallic halide perovskites with different structures. Polyhedral view of crystal structures of $Cs_2AgBiBr_6$,[9] $(C_4H_{12}N)_2CsAgBiBr_7$,[13c] $Cs_4CuSb_2Cl_{12}$,[16] and the new structural type reported in this work.

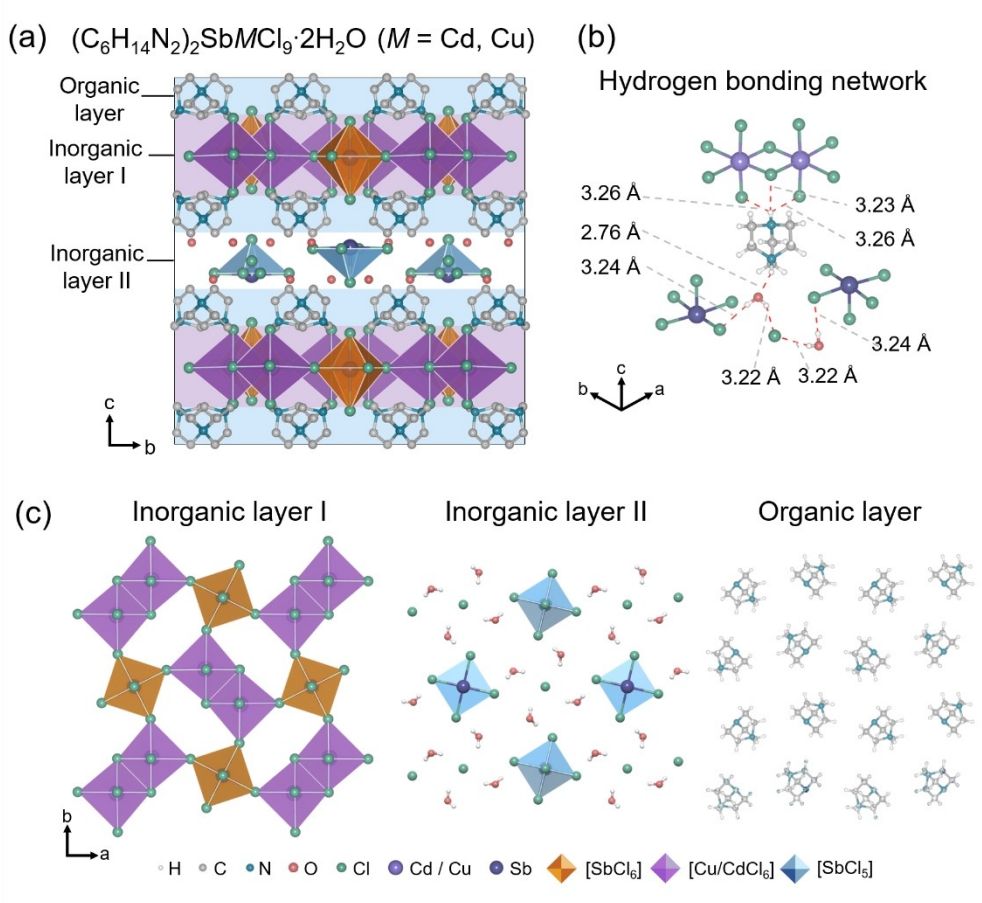

Figure 2. (a) Crystal structure of $(DABCO)_2SbM^{II}Cl_9{\cdot}2H_2O$ (M^{II}=Cd, Cu) viewed along *a*-axis, Sb centered polyhedra are represented in orange and blue, Cd/Cu octahedra are in purple. (b) H-bonding interactions (in red dashes) between inorganic layers and organic layers for SbCd. (c) The structure of different layers in $(DABCO)_2SbM^{II}Cl_9{\cdot}2H_2O$ are viewed along *c*-axis.

$[MCl_6]$ and $[SbCl_6]$. The $[MCl_6]$ octahedra are connected to form binuclear units $[M_2Cl_{10}]$ in an edge-sharing fashion, and the $[M_2Cl_{10}]$ are further corner-shared with the $[SbCl_6]$ octahedra to form a two-dimensional inorganic network. Note that the bridging chlorine between antimony and copper displays site disorder. Furthermore, there is an elongated Sb–Cl bond at ≈2.8 Å, situating perpendicular to the layer, much longer than the usual Sb–Cl bond at ≈2.4 Å. For the zero-dimensional inorganic layer II, there is only one kind of square pyramid $[SbCl_5]$, arranged in an anti-parallel manner along the *c*-axis and staggered along the *b*-axis (the elongated Sb···Cl distances between inorganic layers I and II are greater than 3 Å, and is not considered as a bond[22]). Meanwhile, $[SbCl_5]$ units, crystalline water molecules and free chloride ions are dispersed in this layer via hydrogen bonding. In addition, the antimony species in inorganic layers I and II arranged along the *b*-axis. For the organic layer, due to the hydrogen bonding interaction, one of the ammonium groups of the DABCO cation faces the binuclear units $[M_2Cl_{10}]$, and the other one faces the isolated water molecule. This particular layered structure represents a new structural type in the hybrid metal halide family. We believe that this type of structure can only be achieved with very specific templating cations such as DABCO, which shows certain limitation when trying to expand the family. **SbCd** and **SbCu** have similar Sb–Cl bond lengths and Cl–Sb–Cl bond angles, but the distortion of the $[M^{II}Cl_6]$ octahedra increases when replacing Cd with Cu, which is accompanied by the change of bond length and angle (Tables S2–S4). No obvious Jahn–Teller distortion has been observed in the Cu^{2+} center, which is likely due to the splitting of the Cl atoms in the structure.

To evaluate the optical properties of **SbCd** and **SbCu**, we measured their band gaps and photoluminescence (PL) responses via UV-vis spectroscopy and steady-state PL spectroscopy. As shown in Figure 3, the band gaps of **SbCd** and **SbCu** are determined to be 3.26 and 2.23 eV. The band gap of **SbCd** is similar to that of $Cs_4CdSb_2Cl_{12}$ (3.19 eV)[23] for **SbCd**, while the band gap for **SbCu** is wider than that of $Cs_4CuSb_2Cl_{12}$ (1.02 eV).[16] **SbCu** exhibits a strong absorption peak centered at around 1.5 eV, where we assigned this low energy absorption to the d-d transition of Cu^{2+}.[24]

As shown in Figures 4a and 4c, temperature-dependent PL measurements show that the PL intensity decreases with increasing temperature due to the thermal quenching phenomenon for both **SbCd** and **SbCu**. At 80 K, a broad emission of Sb^{3+} centering at ≈580 nm presented in both compounds. The fitted Huang–Rhys factor of **SbCd** is 47.8

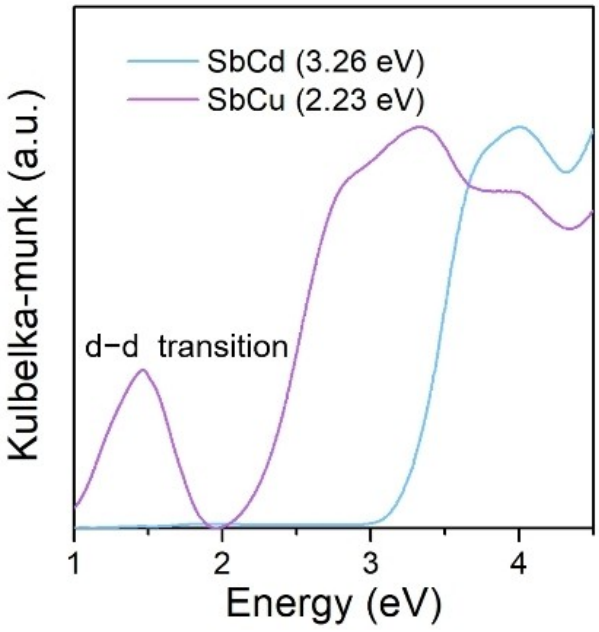

Figure 3. Optical absorption spectra of all compounds at ambient conditions.

(Figure S5), showing a strong coupling strength of electron–phonon coupling, where self-trapped excitonic emission is encouraged.[25] However, no separate emissions of the triplet ($^3P_{0,1,2}$) and singlet ($^1P_1$) states were observed.[25a,26] This result is associated with the symmetry of the crystal structure; high-symmetry structure leads to higher degeneracy of the excited states, so the radiative transition of the singlet state to the ground state $^1S_0$ remains unobserved. According to the above analysis, it is more likely that the broad emission originates from the [$SbCl_6$] species with pseudo-octahedral coordination geometry. For **SbCu**, we identified another obvious dual-band emission at low temperature, with peaks at about 411 and 437 nm. Such blue emission may stem from the $3d^84\ s^1 \rightarrow 3d^9$ transition of Cu^{2+}, which is similar to those reported previously.[27] For the Sb-centered emission, the PL intensity of **SbCd** is stronger than that of **SbCu**, this difference indicates that the partial excitation energy of Sb^{3+} is likely lost during the energy transfer through bridging chlorine to Cu^{2+}, further suggesting that the luminescence of this system originates from the inorganic layer I. As depicted in Figures 4b and 4d, the PL decay curves recorded at different temperatures were measured for both compounds. In most temperature ranges (80–220 K), the lifetime of **SbCd** decreases with increasing temperature, with an unusual increase with higher temperatures than 240 K (Table S5). Such uncommon result[28] is presumably caused by the partially forbidden transitions

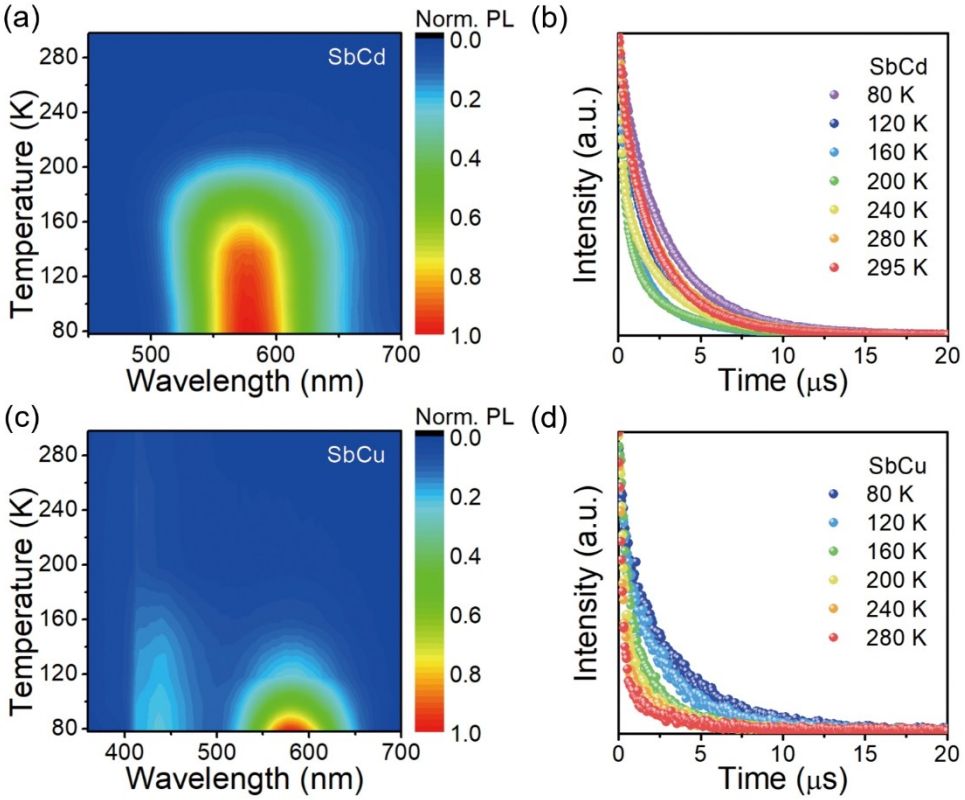

Figure 4. (a) Normalized temperature dependent emission spectrum for SbCd. (b) Time-resolved PL decay spectra for SbCd. (c) Normalized temperature dependent emission spectra for SbCu. (d) Time-resolved PL decay spectra for SbCu.

($^1S_0 \rightarrow {}^3P_{0,1,2}$ and intersystem crossing $^1P_1 \rightarrow {}^3P_{0,1,2}$) related to the splitting of excited states at high temperature. The thermal population of higher energy states ($^3P_0 < {}^3P_1 < {}^3P_2 < {}^1P_1$) of Sb increases at high temperature, resulting in a decrease in the degeneracy of energy levels. These partially forbidden transitions may lead to longer PL decays. However, the PL lifetime of **SbCu** decreases throughout the heating process (Table S6), which may be related to the fact that the PL is more dominated by the Cu center at higher temperatures.

In such complex systems, pressure was employed as an effective stimulus to further tune their optical properties. For **SbCd** and **SbCu**, in situ PL and absorption spectroscopy measurements were carried out under compression. With increasing pressure, the absorption edge of **SbCd** shows a continuous red shift up to ≈19 GPa, followed by a slight blue shift (Figure 5a). We also observed the same continuous red shift of the absorption edge for **SbCu**, while the absorption peak of the *d-d* transition exhibits a blue shift and eventually merges with the absorption edge upon compression (Figure 5b), where the pressure-induced blue shift of d-d band is previously observed.[29] In addition, **SbCd** shows the pressure-dependent emission property (Figure S7). The PL peak exhibits a red shift before ≈10 GPa, and shows a blue shift after ≈10 GPa. The PL intensity decreases first, then increases and reaches its maximum at ≈19 GPa (≈11×initial intensity) (Figures 5c and 5d). After that, the emission intensity starts to weaken, this weakening node coincides with the pressure point where the absorption edge starts to blue shift. Meanwhile, pressure-dependent emission for **SbCd** is reversible while reducing the pressure (Figure S6). However, **SbCu** does not exhibit pressure-induced emission (Figures S8 and S9), which could be due to its already weaker PL emission compared to **SbCd**. Pressure-induced structural variation is probably the main origin of the evolution of these intriguing optical properties for both compounds. Lattice compression changes the orbital overlap between metals and halides, affecting their optoelectronic properties.[18b,30]

To gain a deeper understanding of the electronic structure of **SbCd** and **SbCu**, we performed first-principles calculations within the approximation of density functional theory (DFT). Figure 6 shows the DFT electronic band structures. The calculated electronic band gap for **SbCd** is 2.84 eV (indirect Γ-M). However, for **SbCu**, the open-shell nature of the Cu^{2+} ([Ar]4 $s^2 3d^9$), introduces a magnetic sensitivity to its band structure. To comprehensively understand this impact, both ferromagnetic (FM) and antiferromagnetic (AFM) orderings of **SbCu** are computed and analyzed. As illustrated in Figure S10, despite a marginal energy difference of ≈29 meV/f.u. between FM and AFM, their electronic band structures exhibit notable distinctions, particularly at around 0.5 eV. Notably, the more stable AFM ordering has a band gap of 0.39 eV (indirect Γ-M).

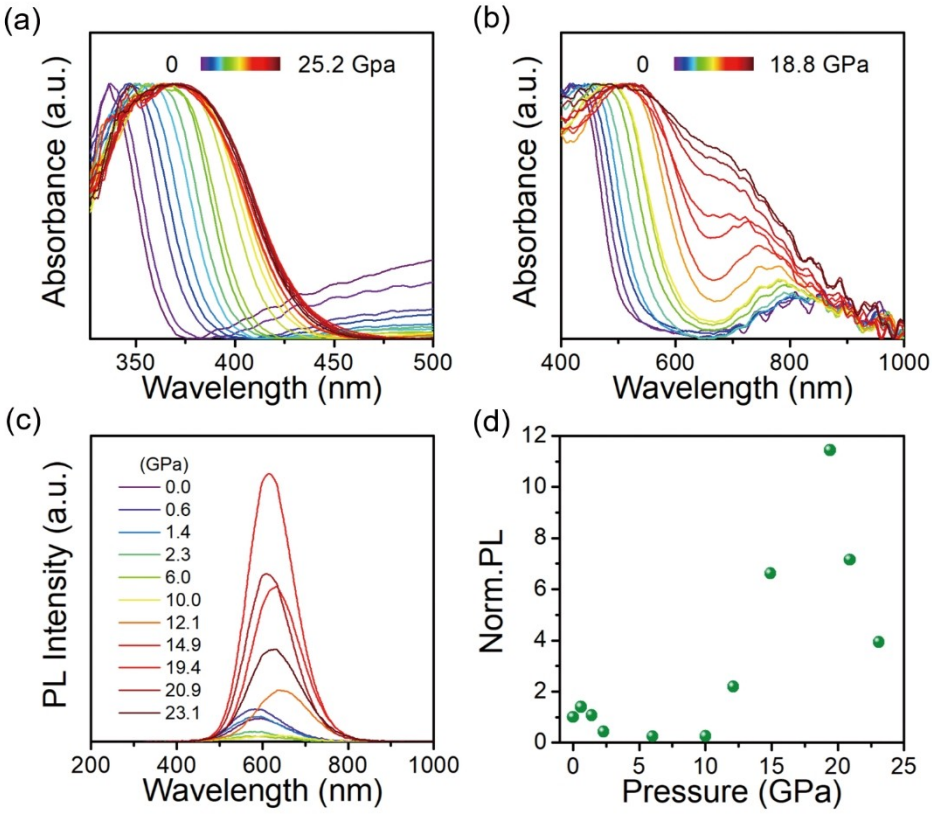

Figure 5. (a) Optical absorption spectra for SbCd at high pressure. (b) Optical absorption spectra for SbCu at high pressure. (c) Emission spectra for SbCd at elevated pressure. (d) Normalized PL intensity at different pressure for SbCd.

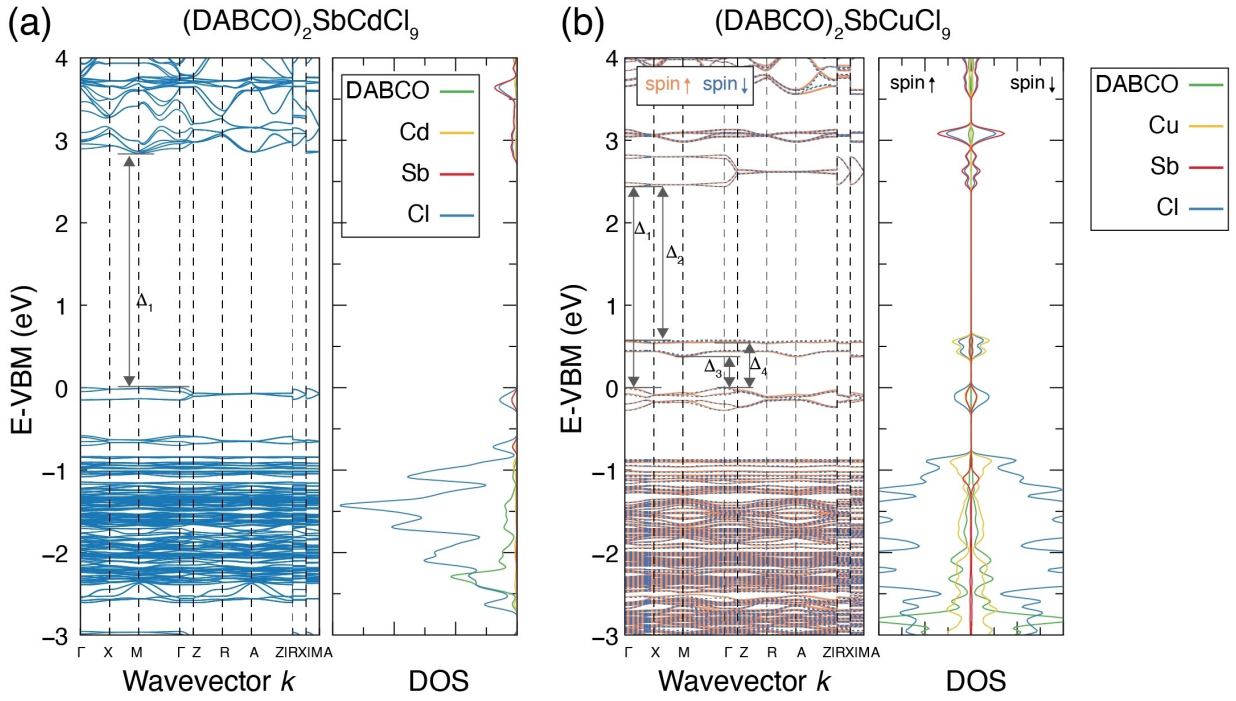

Figure 6. (a) First-principles band structures and projected density of states (pDOS) of SbCd. (b) DFT calculated band structure and projected density of states (pDOS) of SbCu (antiferromagnetic ordering). DFT + U and spin-polarized calculation were applied for SbCu. The valence band maximum (VBM) has been set as 0. The electronic band gap of SbCd (a) and SbCu (antiferromagnetic) (b) have been identified as 2.84 eV (Γ to M) and 0.39 eV (Γ to M), respectively. However, CuSb phase has an invariant energy gap $\Delta_1 = 2.43$ eV (Γ to Γ) regardless of magnetic ordering. Other energy gaps labelled as Δ_1 to Δ_4 are listed in Table S9. A comparison between the band structures of ferromagnetic and antiferromagnetic ordering of SbCu are shown in Figure S10.

However, at room temperature, the magnetic ordering transitions to a paramagnetic state, resulting in continuous fluctuations in the energy states around 0.5 eV due to the disordering of the magnetic structure. However, Δ_1 ($\approx$2.43 eV as shown in Figure 6) remains almost invariant regardless of magnetic ordering, in agreement with the experimental observations. Moreover, the calculated band gaps also follow the trend of the experimental values with values of 3.26 eV and 2.23 eV for Cd and Cu compounds, respectively. The band structures of both compounds display flat dispersions, suggesting high effective masses and limited charge carrier mobility.

Conclusion

In conclusion, we have successfully synthesized two new hybrid bimetallic halides **SbCd** and **SbCu** with a rare 2D layered structure consisting of 0D pyrimads and 2D inorganic layers, sandwiched by DABCO cations. By replacing Cd with Cu, these materials exhibit tunable band gaps and emission properties at room temperature and low temperature. Furthermore, an 11 times enhancement of PL emission is observed at $\approx$19 GPa for **SbCd**, demonstrating that it could serve as a potential candidate for pressure sensing and information storage. This work provides a new example of the hybrid complex bimetallic metal halides and showcases the property tuning via pressure.

Supporting Information

This material is available free of charge via the Internet at http://pubs.acs.org. Detailed experimental procedures, crystal structure data, and computational details.

Acknowledgements

This work was supported by the National Natural Science Foundation of China (NSFC) under Grant Nos. 22275077 and 22275004, the Stable Support Plan Program of Shenzhen Natural Science Fund (Program Contract No. 20220814233319001), and the Startup Fund of SUSTech. The authors are grateful to the assistance of SUSTech Core Research Facilities. P. C. acknowledges support from the Singa-pore Ministry of Education Academic Fund Tier 1 (R-284-000-186-133). The computational work for this article was partially performed on resources of the National Supercomputing Centre, Singapore (https://www.nscc.sg). Z. D. acknowledges the support from his Lee Kuan Yew Postdoctoral Fellowship 22-5930-A0001. The authors thank Dr. Jiawei Lin for his help in analyzing the experimental data.

Conflict of Interest

The authors declare no conflict of interest.

Data Availability Statement

The data that support the findings of this study are available from the corresponding author upon reasonable request.

Keywords: Electronic Properties · Hybrid Metal Halide · Perovskite Derivatives · Photoluminescence · Pressure

[1] a) J. Y. Kim, J.-W. Lee, H. S. Jung, H. Shin, N.-G. Park, *Chem. Rev.* **2020**, *120*, 7867–7918; b) A. Kojima, K. Teshima, Y. Shirai, T. Miyasaka, *J. Am. Chem. Soc.* **2009**, *131*, 6050–6051.

[2] a) S. D. Stranks, H. J. Snaith, *Nat. Nanotechnol.* **2015**, *10*, 391–402; b) M. Yuan, L. N. Quan, R. Comin, G. Walters, R. Sabatini, O. Voznyy, S. Hoogland, Y. Zhao, E. M. Beauregard, P. Kanjanaboos, Z. Lu, D. H. Kim, E. H. Sargent, *Nat. Nanotechnol.* **2016**, *11*, 872–877.

[3] a) H. Zhu, Y. Fu, F. Meng, X. Wu, Z. Gong, Q. Ding, M. V. Gustafsson, M. T. Trinh, S. Jin, X. Y. Zhu, *Nat. Mater.* **2015**, *14*, 636–642; b) Y. Jia, R. A. Kerner, A. J. Grede, B. P. Rand, N. C. Giebink, *Nat. Photonics* **2017**, *11*, 784–788.

[4] a) B. Saparov, D. B. Mitzi, *Chem. Rev.* **2016**, *116*, 4558–4596; b) L. Mao, C. C. Stoumpos, M. G. Kanatzidis, *J. Am. Chem. Soc.* **2019**, *141*, 1171–1190.

[5] a) Z. Xiao, Z. Song, Y. Yan, *Adv. Mater.* **2019**, *31*, 1803792; b) A. Babayigit, A. Ethirajan, M. Muller, B. Conings, *Nat. Mater.* **2016**, *15*, 247–251.

[6] a) M. Pitaro, E. K. Tekelenburg, S. Shao, M. A. Loi, *Adv. Mater.* **2022**, *34*, 2105844; b) Y. Liu, Y.-P. Gong, S. Geng, M.-L. Feng, D. Manidaki, Z. Deng, C. C. Stoumpos, P. Canepa, Z. Xiao, W.-X. Zhang, L. Mao, *Angew. Chem. Int. Ed.* **2022**, *61*, e202208875; c) C. Chen, X. Zhao, Y. Gong, Y. Liu, Z. Chen, L. Zhang, J. Chen, Z. Deng, H. Lu, M. Luo, P. Canepa, L. Mao, *Chem. Mater.* **2023**, *35*, 3265–3275; d) X. Li, Y. Guan, X. Li, Y. Fu, *J. Am. Chem. Soc.* **2022**, *144*, 18030–18042.

[7] a) J. Zhou, P. Xie, C. Wang, T. Bian, J. Chen, Y. Liu, Z. Guo, C. Chen, X. Pan, M. Luo, J. Yin, L. Mao, *Angew. Chem. Int. Ed.* **2023**, *62*, e202307646; b) F. Wei, Z. Deng, S. Sun, F. Zhang, D. M. Evans, G. Kieslich, S. Tominaka, M. A. Carpenter, J. Zhang, P. D. Bristowe, A. K. Cheetham, *Chem. Mater.* **2017**, *29*, 1089–1094; c) L. R. Morss, M. Siegal, L. Stenger, N. Edelstein, *Inorg. Chem.* **1970**, *9*, 1771–1775; d) Z. Deng, F. Wei, S. Sun, G. Kieslich, A. K. Cheetham, P. D. Bristowe, *J. Mater. Chem. A* **2016**, *4*, 12025–12029; e) N. Elliott, L. Pauling, *J. Am. Chem. Soc.* **1938**, *60*, 1846–1851; f) F. Wei, Z. Deng, S. Sun, F. Xie, G. Kieslich, D. M. Evans, M. A. Carpenter, P. D. Bristowe, A. K. Cheetham, *Mater. Horiz.* **2016**, *3*, 328–332; g) G. Meyer, H.-C. Gaebell, *Z. Naturforsch. B* **1978**, *33*, 1476–1478.

[8] H. L. Wells, *Am. J. Sci.* **1922**, *s5-4*, 476–482.

[9] A. H. Slavney, T. Hu, A. M. Lindenberg, H. I. Karunadasa, *J. Am. Chem. Soc.* **2016**, *138*, 2138–2141.

[10] E. T. McClure, M. R. Ball, W. Windl, P. M. Woodward, *Chem. Mater.* **2016**, *28*, 1348–1354.

[11] T. T. Tran, J. R. Panella, J. R. Chamorro, J. R. Morey, T. M. McQueen, *Mater. Horiz.* **2017**, *4*, 688–693.

[12] G. Volonakis, A. A. Haghighirad, R. L. Milot, W. H. Sio, M. R. Filip, B. Wenger, M. B. Johnston, L. M. Herz, H. J. Snaith, F. Giustino, *J. Phys. Chem. Lett.* **2017**, *8*, 772–778.

[13] a) B. Vargas, G. Rodríguez-López, D. Solis-Ibarra, *ACS Energy Lett.* **2020**, *5*, 3591–3608; b) H. A. Evans, L. Mao, R. Seshadri, A. K. Cheetham, *Annu. Rev. Mater. Res.* **2021**, *51*, 351–380; c) B. A. Connor, L. Leppert, M. D. Smith, J. B. Neaton, H. I. Karunadasa, *J. Am. Chem. Soc.* **2018**, *140*, 5235–5240.

[14] M. K. Jana, S. M. Janke, D. J. Dirkes, S. Dovletgeldi, C. Liu, X. Qin, K. Gundogdu, W. You, V. Blum, D. B. Mitzi, *J. Am. Chem. Soc.* **2019**, *141*, 7955–7964.

[15] a) E. T. McClure, A. P. McCormick, P. M. Woodward, *Inorg. Chem.* **2020**, *59*, 6010–6017; b) L.-Y. Bi, Y.-Q. Hu, M.-Q. Li, T.-L. Hu, H.-L. Zhang, X.-T. Yin, W.-X. Que, M. S. Lassoued, Y.-Z. Zheng, *J. Mater. Chem. A* **2019**, *7*, 19662–19667; c) M. S. Lassoued, L.-Y. Bi, Z. Wu, G. Zhou, Y.-Z. Zheng, *J. Mater. Chem. C* **2020**, *8*, 5349–5354; d) L. Mao, S. M. L. Teicher, C. C. Stoumpos, R. M. Kennard, R. A. DeCrescent, G. Wu, J. A. Schuller, M. L. Chabinyc, A. K. Cheetham, R. Seshadri, *J. Am. Chem. Soc.* **2019**, *141*, 19099–19109.

[16] B. Vargas, E. Ramos, E. Pérez-Gutiérrez, J. C. Alonso, D. Solis-Ibarra, *J. Am. Chem. Soc.* **2017**, *139*, 9116–9119.

[17] a) B. Vargas, D. T. Reyes-Castillo, E. Coutino-Gonzalez, C. Sánchez-Aké, C. Ramos, C. Falcony, D. Solis-Ibarra, *Chem. Mater.* **2020**, *32*, 9307–9315; b) B. Vargas, R. Torres-Cadena, J. Rodríguez-Hernández, M. Gembicky, H. Xie, J. Jiménez-Mier, Y.-S. Liu, E. Menéndez-Proupin, K. R. Dunbar, N. Lopez, P. Olalde-Velasco, D. Solis-Ibarra, *Chem. Mater.* **2018**, *30*, 5315–5321; c) B. Vargas, E. Coutiño-Gonzalez, O. Ovalle-Encinia, C. Sánchez-Aké, D. Solis-Ibarra, *J. Phys. Chem. Lett.* **2020**, *11*, 10362–10367.

[18] a) A. Jaffe, Y. Lin, C. M. Beavers, J. Voss, W. L. Mao, H. I. Karunadasa, *ACS Cent. Sci.* **2016**, *2*, 201–209; b) L. Zhang, S. Li, H. Sun, Q. Jiang, Y. Wang, Y. Fang, Y. Shi, D. Duan, K. Wang, H. Jiang, L. Sui, G. Wu, K. Yuan, B. Zou, *Angew. Chem. Int. Ed.* **2023**, *62*, e202301573; c) T. Fu, K. Bu, X. Sun, D. Wang, X. Feng, S. Guo, Z. Sun, Y. Fang, Q. Hu, Y. Ding, T. Zhai, F. Huang, X. Lü, *J. Am. Chem. Soc.* **2023**, *145*, 16828–16834; d) K. Bu, Q. Hu, X. Qi, D. Wang, S. Guo, H. Luo, T. Lin, X. Guo, Q. Zeng, Y. Ding, F. Huang, W. Yang, H.-K. Mao, X. Lü, *Nat. Commun.* **2022**, *13*, 4650.

[19] Y. Fang, L. Zhang, L. Wu, J. Yan, Y. Lin, K. Wang, W. L. Mao, B. Zou, *Angew. Chem. Int. Ed.* **2019**, *58*, 15249–15253.

[20] H. Yang, W. Shi, Y. Nagaoka, Z. Liu, R. Li, O. Chen, *J. Phys. Chem. C* **2023**, *127*, 2407–2415.

[21] Deposition numbers 2285462 (for SbCd), and 2285463 (for SbCd) contain the supplementary crystallographic data for this paper. These data are provided free of charge by the joint Cambridge Crystallographic Data Centre and Fachinformationszentrum Karlsruhe Access Structures service.

[22] C. Sun, Z. Deng, Z. Li, Z. Chen, X. Zhang, J. Chen, H. Lu, P. Canepa, R. Chen, L. Mao, *Angew. Chem. Int. Ed.* **2023**, *62*, e202216720.

[23] T. Cai, W. Shi, D. J. Gosztola, K. Kobbekaduwa, H. Yang, N. Jin, Y. Nagaoka, L. Dube, J. Schneider, S. Hwang, J. Gao, X. Ma, O. Chen, *Matter* **2021**, *4*, 2936–2952.

[24] M. Ulutagay-Kartin, S.-J. Hwu, J. A. Clayhold, *Inorg. Chem.* **2003**, *42*, 2405–2409.

[25] a) Y. Jing, Y. Liu, M. Li, Z. Xia, *Adv. Opt. Mater.* **2021**, *9*, 2002213; b) B. Yang, L. Yin, G. Niu, J.-H. Yuan, K.-H. Xue, Z. Tan, X.-S. Miao, M. Niu, X. Du, H. Song, E. Lifshitz, J. Tang, *Adv. Mater.* **2019**, *31*, 1904711; c) S. Li, J. Luo, J. Liu, J. Tang, *J. Phys. Chem. Lett.* **2019**, *10*, 1999–2007; d) J. Luo, X. Wang, S. Li, J. Liu, Y. Guo, G. Niu, L. Yao, Y. Fu, L. Gao, Q. Dong, C. Zhao, M. Leng, F. Ma, W. Liang, L. Wang, S. Jin, J. Han, L. Zhang, J. Etheridge, J. Wang, Y. Yan, E. H. Sargent, J. Tang, *Nature* **2018**, *563*, 541–545.

[26] K. M. McCall, V. Morad, B. M. Benin, M. V. Kovalenko, *ACS Materials Lett.* **2020**, *2*, 1218–1232.

[27] a) T. Aidilibike, Y. Li, J. Guo, X. Liu, W. Qin, *J. Mater. Chem. C* **2016**, *4*, 2123–2126; b) C. Bi, S. Wang, Q. Li, S. V. Kershaw, J. Tian, A. L. Rogach, *J. Phys. Chem. Lett.* **2019**, *10*, 943–952.
[28] a) M. Müller, T. Jüstel, *Dalton Trans.* **2015**, *44*, 10368–10376; b) X. Lan, Q. Wei, Y. Chen, W. Tang, *Opt. Mater.* **2012**, *34*, 1330–1332; c) R. Karpicz, N. Ostapenko, Y. Ostapenko, Y. Polupan, I. Lazarev, N. Galunov, M. Macernis, D. Abramavicius, L. Valkunas, *Phys. Chem. Chem. Phys.* **2021**, *23*, 3447–3454.
[29] a) O. S. Wenger, R. Valiente, H. U. Güdel, *J. Chem. Phys.* **2001**, *115*, 3819–3826; b) J. K. Grey, I. S. Butler, C. Reber, *J. Am. Chem. Soc.* **2002**, *124*, 9384–9385.
[30] S. Guo, K. Bu, J. Li, Q. Hu, H. Luo, Y. He, Y. Wu, D. Zhang, Y. Zhao, W. Yang, M. G. Kanatzidis, X. Lü, *J. Am. Chem. Soc.* **2021**, *143*, 2545–2551.

Manuscript received: October 6, 2023
Version of record online: ■■, ■■

Research Articles

Hybrid Metal Halides

Y. Liu, J. Liang, Z. Deng,* S. Guo, X. Ji, C. Chen, P. Canepa, X. Lü,* L. Mao* e202314977

0D Pyramid-intercalated 2D Bimetallic Halides with Tunable Electronic Structures and Enhanced Emission under Pressure

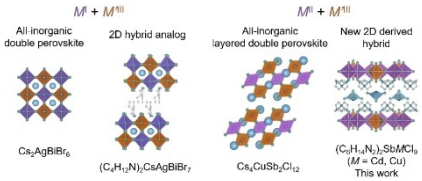

Here, we report a new unique family of hybrid layered bimetallic halides with Cd/Cu as the M^{II} site and Sb as the M^{III} site within the layered structure, with intercalated $SbCl_5$ pyramids. These materials exhibit tunable electronic properties and optical band gaps from 2 to 3 eV. Using pressure as an external stimulus, the photoluminescence of the Cd analog is largely enhanced by 11 times.